7th European Conference on Structural Dynamics
EURODYN 2008
7-9 July 2008 Southampton

DYNAMIC ANALYSIS OF THE TRAIN-BRIDGE INTERACTION: AN ACCURATE AND EFFICIENT NUMERICAL METHOD

Álvaro Azevedo[1]*, Sérgio Neves[2] and Rui Calçada[2]

[1]Department of Civil Engineering
Faculty of Engineering
University of Porto
Rua Dr. Roberto Frias, s/n, 4200-465 Porto, Portugal
E-mail: alvaro@fe.up.pt Web: http://www.fe.up.pt/~alvaro

[2]Department of Civil Engineering
Faculty of Engineering
University of Porto
Rua Dr. Roberto Frias, s/n, 4200-465 Porto, Portugal
E-mail: {sgneves,ruiabc}@fe.up.pt Web: http://www.fe.up.pt

Keywords: Train-bridge interaction, dynamic analysis, HHT method, finite element method.

ABSTRACT

The dynamic behavior of railway bridges carrying high-speed trains can be analyzed with or without the consideration of the vehicle's own structure. However, due to the amount of kinetic energy carried at high speeds, the train may interact significantly with the bridge, especially when resonance occurs. Equally important is the riding comfort and the stability of the track and train cars, which are usually the most critical limit states in the design of this type of structures. With the aim of studying this problem a computer code was developed, being the interaction between the bridge and the train implemented by means of contact conditions between each train wheel (nodal point) and the structure (point inside a finite element). The treatment of the interaction between a train wheel and a point on the surface of a finite element is directly and efficiently implemented by means of an extended stiffness matrix, which includes stiffness, flexibility and additional terms that stem from the compatibility equations between the displacements of the vehicle and the bridge. This methodology was applied to the study of the dynamic behavior of a bowstring arch bridge and proved to be very accurate and efficient.

2. INTRODUCTION

The dynamic behavior of railway bridges carrying high-speed trains can be analyzed with or without the consideration of the vehicle's own structure. The simulation of the train-bridge system requires several independent submeshes and the consideration of contact conditions that represent their interaction.

Delgado and Cruz [1] and Calçada [2] developed a computational methodology to analyze the train-bridge interaction. This methodology was implemented in a previous version of FEMIX, which is a general purpose finite element computer program [3]. The developed algorithm is very versatile, allowing the modeling of any structure and vehicle using 3D beam elements. However the treatment of the contact conditions between the independent submeshes is performed by an iterative process, which can be inefficient.

This paper describes the formulation of the contact between nodal points of the vehicle and internal points of a finite element. Dynamic equilibrium equations in non prescribed degrees of freedom, in contact degrees of freedom and in prescribed degrees of freedom are separately developed. Contact compatibility equations between points of the vehicle and internal points of a finite element are also separately developed. All these equations constitute a single system of linear equations involving displacements, contact forces and reactions as unknowns. After the solution of this system of linear equations the displacements, velocities and accelerations at the current time step can be calculated and a new time step is started. This heterogeneous system of linear equations can be efficiently solved by means of the consideration of several submatrices with specific characteristics.

The new formulation described here is applied to the analysis of the dynamic behavior of the São Lourenço bridge, which is a bowstring arch bridge. The bridge is located in the North Line of the Portuguese railway system, in a section that was recently upgraded to allow the passage of the Alfa pendular train at greater speeds. The numerical model was validated with the results of the ambient vibration test and those measured during several passages of the Alfa pendular train. The dynamic response of the train-bridge system was calculated for train speeds exceeding the allowable speed for that section of the North Line.

2. HHT METHOD WITH TRAIN-BRIDGE INTERACTION

A simple example is used to introduce the types of degrees of freedom that are considered in the formulation of the vehicle-structure interaction in the context of a time step of the Hilber-Hughes-Taylor method (see Figure 1). On the right, a simply supported beam with two spans ($B1$ and $B2$) is subjected to the contact of a vehicle, shown on the left. The structure of the vehicle is also composed of two beams ($B3$ and $B4$). Nodes 7, 8 and 9 are internal points of the beam $B1$. The location of these nodes may change between time steps, depending on the position of the vehicle. Eventual gaps between both structures (g_i) can be easily considered in the compatibility equations, as will be shown later.

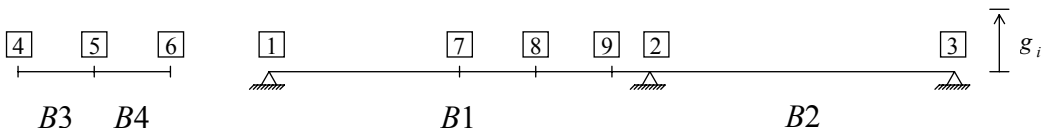

Figure 1. Vehicle and structure: beams and nodal points

In each nodal point two degrees of freedom are considered (vertical displacement and

rotation). Figure 2 shows the generalized displacements in nodal points (1 to 12), the generalized displacements of the contact points of the structure (13, 14 and 15), the interaction forces in the vehicle (X_7, X_9 and X_{11}) and the interaction forces in the structure (Y_{13}, Y_{14} and Y_{15}). The interaction only involves the translational degrees of freedom.

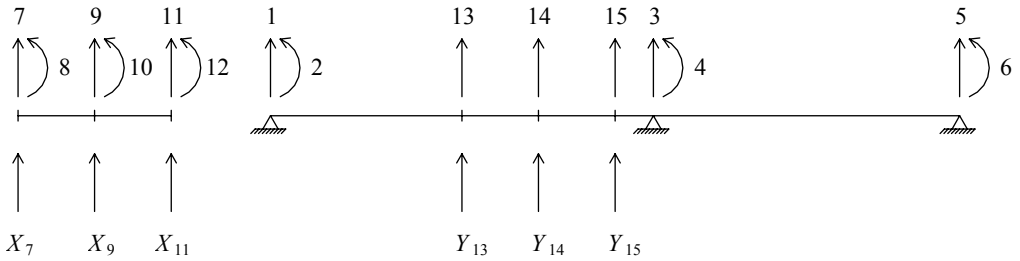

Figure 2. Vehicle and structure: degrees of freedom and interactions forces

The following classification of the degrees of freedom is considered:

- F – free;
- X – interaction (vehicle);
- P – prescribed;
- Y – interaction (structure).

This classification is used later in this section.

In the context of the Hilber-Hughes-Taylor method (HHT), the dynamic equilibrium equation that involves the degrees of freedom in nodal points (1 to 12) is the following

$$\underline{\mathbf{M}}\,\underline{\ddot{\mathbf{u}}}^{c} + (1+\alpha)\,\underline{\mathbf{C}}\,\underline{\dot{\mathbf{u}}}^{c} - \alpha\,\underline{\mathbf{C}}\,\underline{\dot{\mathbf{u}}}^{p} + (1+\alpha)\,\underline{\mathbf{K}}\,\underline{\mathbf{u}}^{c} - \alpha\,\underline{\mathbf{K}}\,\underline{\mathbf{u}}^{p} = (1+\alpha)\,\underline{\mathbf{F}}^{c} - \alpha\underline{\mathbf{F}}^{p} \tag{1}$$

In this equation $\underline{\mathbf{M}}$ is the mass matrix, $\underline{\mathbf{C}}$ is the damping matrix, $\underline{\mathbf{K}}$ is the stiffness matrix, $\underline{\mathbf{F}}$ are the applied generalized forces, $\underline{\mathbf{u}}$ are the generalized displacements and α is the main parameter of the HHT method. When $\alpha = 0$ the HHT method reduces to the Newmark method, and for other values of the parameter α, numerical energy dissipation is introduced in the higher modes. The superscript c indicates the current time step ($t + \Delta t$) and the superscript p indicates the previous one (t).

According to Figure 2 and to the classification indicated above, the F type degrees of freedom are the following: 2, 4, 6, 8, 10 and 12. The X type degrees of freedom correspond to the "supports" of the separated vehicle structure, being the following: 7, 9 and 11. The P type degrees of freedom are the main structural supports 1, 3 and 5. The Y type degrees of freedom 13, 14 and 15 consist on the internal displacements of beam $B1$ at the contact points.

According to this classification of degrees of freedom, Eq. (1) can be expanded by considering several submatrices, yielding

$$\begin{bmatrix} \underline{\mathbf{M}}_{FF} & \underline{\mathbf{M}}_{FX} & \underline{\mathbf{M}}_{FP} \\ \underline{\mathbf{M}}_{XF} & \underline{\mathbf{M}}_{XX} & \underline{\mathbf{M}}_{XP} \\ \underline{\mathbf{M}}_{PF} & \underline{\mathbf{M}}_{PX} & \underline{\mathbf{M}}_{PP} \end{bmatrix} \begin{bmatrix} \ddot{\underline{\mathbf{u}}}_F^c \\ \ddot{\underline{\mathbf{u}}}_X^c \\ \ddot{\underline{\mathbf{u}}}_P^c \end{bmatrix} \tag{2}$$

$$+(1+\alpha) \begin{bmatrix} \underline{\mathbf{C}}_{FF} & \underline{\mathbf{C}}_{FX} & \underline{\mathbf{C}}_{FP} \\ \underline{\mathbf{C}}_{XF} & \underline{\mathbf{C}}_{XX} & \underline{\mathbf{C}}_{XP} \\ \underline{\mathbf{C}}_{PF} & \underline{\mathbf{C}}_{PX} & \underline{\mathbf{C}}_{PP} \end{bmatrix} \begin{bmatrix} \dot{\underline{\mathbf{u}}}_F^c \\ \dot{\underline{\mathbf{u}}}_X^c \\ \dot{\underline{\mathbf{u}}}_P^c \end{bmatrix} - \alpha \begin{bmatrix} \underline{\mathbf{C}}_{FF} & \underline{\mathbf{C}}_{FX} & \underline{\mathbf{C}}_{FP} \\ \underline{\mathbf{C}}_{XF} & \underline{\mathbf{C}}_{XX} & \underline{\mathbf{C}}_{XP} \\ \underline{\mathbf{C}}_{PF} & \underline{\mathbf{C}}_{PX} & \underline{\mathbf{C}}_{PP} \end{bmatrix} \begin{bmatrix} \dot{\underline{\mathbf{u}}}_F^p \\ \dot{\underline{\mathbf{u}}}_X^p \\ \dot{\underline{\mathbf{u}}}_P^p \end{bmatrix}$$

$$+(1+\alpha) \begin{bmatrix} \underline{\mathbf{K}}_{FF} & \underline{\mathbf{K}}_{FX} & \underline{\mathbf{K}}_{FP} \\ \underline{\mathbf{K}}_{XF} & \underline{\mathbf{K}}_{XX} & \underline{\mathbf{K}}_{XP} \\ \underline{\mathbf{K}}_{PF} & \underline{\mathbf{K}}_{PX} & \underline{\mathbf{K}}_{PP} \end{bmatrix} \begin{bmatrix} \underline{\mathbf{u}}_F^c \\ \underline{\mathbf{u}}_X^c \\ \underline{\mathbf{u}}_P^c \end{bmatrix} - \alpha \begin{bmatrix} \underline{\mathbf{K}}_{FF} & \underline{\mathbf{K}}_{FX} & \underline{\mathbf{K}}_{FP} \\ \underline{\mathbf{K}}_{XF} & \underline{\mathbf{K}}_{XX} & \underline{\mathbf{K}}_{XP} \\ \underline{\mathbf{K}}_{PF} & \underline{\mathbf{K}}_{PX} & \underline{\mathbf{K}}_{PP} \end{bmatrix} \begin{bmatrix} \underline{\mathbf{u}}_F^p \\ \underline{\mathbf{u}}_X^p \\ \underline{\mathbf{u}}_P^p \end{bmatrix} =$$

$$(1+\alpha) \begin{bmatrix} \underline{\mathbf{P}}_F^c + \underline{\mathbf{d}}_{FY}\ \underline{\mathbf{Y}}_Y^c \\ \underline{\mathbf{P}}_X^c + \underline{\mathbf{I}}_{XX}\ \underline{\mathbf{X}}_X^c \\ \underline{\mathbf{P}}_P^c + \underline{\mathbf{d}}_{PY}\ \underline{\mathbf{Y}}_Y^c + \underline{\mathbf{R}}_P^c \end{bmatrix} - \alpha \begin{bmatrix} \underline{\mathbf{P}}_F^p + \underline{\mathbf{d}}_{FY}\ \underline{\mathbf{Y}}_Y^p \\ \underline{\mathbf{P}}_X^p + \underline{\mathbf{I}}_{XX}\ \underline{\mathbf{X}}_X^p \\ \underline{\mathbf{P}}_P^p + \underline{\mathbf{d}}_{PY}\ \underline{\mathbf{Y}}_Y^p + \underline{\mathbf{R}}_P^p \end{bmatrix}$$

In the F type degrees of freedom,

$$\underline{\mathbf{F}}_F = \underline{\mathbf{P}}_F + \underline{\mathbf{d}}_{FY}\ \underline{\mathbf{Y}}_Y \tag{3}$$

being $\underline{\mathbf{P}}$ the external loads applied in correspondence with each degree of freedom. Each component d_{ij} of $\underline{\mathbf{d}}_{FY}$ corresponds to the nodal force in the F type degree of freedom i, which is equivalent to a single load consisting of a unitary value of Y_j (see Figure 2).

In the X type degrees of freedom,

$$\underline{\mathbf{F}}_X = \underline{\mathbf{P}}_X + \underline{\mathbf{I}}_{XX}\ \underline{\mathbf{X}}_X \tag{4}$$

being $\underline{\mathbf{I}}_{XX}$ the identity matrix with an appropriate size.

In the P type degrees of freedom,

$$\underline{\mathbf{F}}_P = \underline{\mathbf{P}}_P + \underline{\mathbf{d}}_{PY}\ \underline{\mathbf{Y}}_Y + \underline{\mathbf{R}}_P \tag{5}$$

being $\underline{\mathbf{R}}_P$ the reactions.

According to Figure 2, equilibrium equations in the contact degrees of freedom can be written, yielding

$$\underline{\mathbf{Y}}_Y = -\underline{\mathbf{X}}_X \tag{6}$$

Since the number of Y type degrees of freedom coincides with the number of X type degrees of freedom, the subscript Y may be replaced with X.

According to [4], Eq. (2) is equivalent to the following three equations

$$\overline{\underline{\mathbf{K}}}_{FF}\underline{\mathbf{u}}_F^c + \overline{\underline{\mathbf{K}}}_{FX}\underline{\mathbf{u}}_X^c + (1+\alpha)\underline{\mathbf{d}}_{FX}\ \underline{\mathbf{X}}_X^c = \overline{\underline{\mathbf{F}}}_F \tag{7}$$

$$\overline{\underline{\mathbf{K}}}_{XF}\,\underline{\mathbf{u}}_F^c+\overline{\underline{\mathbf{K}}}_{XX}\,\underline{\mathbf{u}}_X^c-(1+\alpha)\,\underline{\mathbf{I}}_{XX}\,\underline{\mathbf{X}}_X^c=\overline{\underline{\mathbf{F}}}_X \tag{8}$$

$$\begin{aligned}\underline{\mathbf{R}}_P^c=&\frac{\alpha}{1+\alpha}\,\underline{\mathbf{R}}_P^p-\underline{\mathbf{P}}_P^c+\frac{\alpha}{1+\alpha}\,\underline{\mathbf{P}}_P^p+\underline{\mathbf{d}}_{PX}\,\underline{\mathbf{X}}_X^c-\frac{\alpha}{1+\alpha}\,\underline{\mathbf{d}}_{PX}\,\underline{\mathbf{X}}_X^p\\&+\frac{1}{1+\alpha}\underline{\mathbf{M}}_{PF}\,\ddot{\underline{\mathbf{u}}}_F^c+\frac{1}{1+\alpha}\underline{\mathbf{M}}_{PX}\,\ddot{\underline{\mathbf{u}}}_X^c+\frac{1}{1+\alpha}\underline{\mathbf{M}}_{PP}\ddot{\underline{\mathbf{u}}}_P^c\\&+\underline{\mathbf{C}}_{PF}\,\dot{\underline{\mathbf{u}}}_F^c+\underline{\mathbf{C}}_{PX}\,\dot{\underline{\mathbf{u}}}_X^c+\underline{\mathbf{C}}_{PP}\,\dot{\underline{\mathbf{u}}}_P^c-\frac{\alpha}{1+\alpha}\,\underline{\mathbf{C}}_{PF}\,\dot{\underline{\mathbf{u}}}_F^p-\frac{\alpha}{1+\alpha}\,\underline{\mathbf{C}}_{PX}\,\dot{\underline{\mathbf{u}}}_X^p-\frac{\alpha}{1+\alpha}\,\underline{\mathbf{C}}_{PP}\,\dot{\underline{\mathbf{u}}}_P^p\\&+\underline{\mathbf{K}}_{PF}\,\underline{\mathbf{u}}_F^c+\underline{\mathbf{K}}_{PX}\,\underline{\mathbf{u}}_X^c+\underline{\mathbf{K}}_{PP}\,\underline{\mathbf{u}}_P^c-\frac{\alpha}{1+\alpha}\,\underline{\mathbf{K}}_{PF}\,\underline{\mathbf{u}}_F^p-\frac{\alpha}{1+\alpha}\,\underline{\mathbf{K}}_{PX}\,\underline{\mathbf{u}}_X^p-\frac{\alpha}{1+\alpha}\,\underline{\mathbf{K}}_{PP}\,\underline{\mathbf{u}}_P^p\end{aligned} \tag{9}$$

being

$$\overline{\underline{\mathbf{K}}}_{FF}=A_0\underline{\mathbf{M}}_{FF}+(1+\alpha)\,A_1\underline{\mathbf{C}}_{FF}+(1+\alpha)\underline{\mathbf{K}}_{FF} \tag{10}$$

$$\overline{\underline{\mathbf{K}}}_{FX}=A_0\underline{\mathbf{M}}_{FX}+(1+\alpha)\,A_1\underline{\mathbf{C}}_{FX}+(1+\alpha)\underline{\mathbf{K}}_{FX}$$

$$\overline{\underline{\mathbf{K}}}_{XF}=A_0\underline{\mathbf{M}}_{XF}+(1+\alpha)\,A_1\underline{\mathbf{C}}_{XF}+(1+\alpha)\underline{\mathbf{K}}_{XF}$$

$$\overline{\underline{\mathbf{K}}}_{XX}=A_0\underline{\mathbf{M}}_{XX}+(1+\alpha)\,A_1\underline{\mathbf{C}}_{XX}+(1+\alpha)\underline{\mathbf{K}}_{XX}$$

$$\begin{aligned}\overline{\underline{\mathbf{F}}}_F=&(1+\alpha)\,\underline{\mathbf{P}}_F^c-\alpha\,\underline{\mathbf{P}}_F^p+\alpha\,\underline{\mathbf{d}}_{FX}\,\underline{\mathbf{X}}_X^p-\underline{\mathbf{M}}_{FP}\ddot{\underline{\mathbf{u}}}_P^c\\&-(1+\alpha)\,\underline{\mathbf{C}}_{FP}\,\dot{\underline{\mathbf{u}}}_P^c+\alpha\,\underline{\mathbf{C}}_{FF}\,\dot{\underline{\mathbf{u}}}_F^p+\alpha\,\underline{\mathbf{C}}_{FX}\,\dot{\underline{\mathbf{u}}}_X^p+\alpha\,\underline{\mathbf{C}}_{FP}\,\dot{\underline{\mathbf{u}}}_P^p\\&-(1+\alpha)\,\underline{\mathbf{K}}_{FP}\,\underline{\mathbf{u}}_P^c+\alpha\,\underline{\mathbf{K}}_{FF}\,\underline{\mathbf{u}}_F^p+\alpha\,\underline{\mathbf{K}}_{FX}\,\underline{\mathbf{u}}_X^p+\alpha\,\underline{\mathbf{K}}_{FP}\,\underline{\mathbf{u}}_P^p\\&+\underline{\mathbf{M}}_{FF}\left[A_0\,\underline{\mathbf{u}}_F^p+A_2\,\dot{\underline{\mathbf{u}}}_F^p+A_3\,\ddot{\underline{\mathbf{u}}}_F^p\right]+\underline{\mathbf{M}}_{FX}\left[A_0\,\underline{\mathbf{u}}_X^p+A_2\,\dot{\underline{\mathbf{u}}}_X^p+A_3\,\ddot{\underline{\mathbf{u}}}_X^p\right]\\&+(1+\alpha)\,\underline{\mathbf{C}}_{FF}\left[A_1\,\underline{\mathbf{u}}_F^p+A_4\,\dot{\underline{\mathbf{u}}}_F^p+A_5\,\ddot{\underline{\mathbf{u}}}_F^p\right]+(1+\alpha)\,\underline{\mathbf{C}}_{FX}\left[A_1\,\underline{\mathbf{u}}_X^p+A_4\,\dot{\underline{\mathbf{u}}}_X^p+A_5\,\ddot{\underline{\mathbf{u}}}_X^p\right]\end{aligned} \tag{11}$$

$$\begin{aligned}\overline{\underline{\mathbf{F}}}_X=&(1+\alpha)\,\underline{\mathbf{P}}_X^c-\alpha\,\underline{\mathbf{P}}_X^p-\alpha\,\underline{\mathbf{I}}_{XX}\,\underline{\mathbf{X}}_X^p-\underline{\mathbf{M}}_{XP}\ddot{\underline{\mathbf{u}}}_P^c\\&-(1+\alpha)\,\underline{\mathbf{C}}_{XP}\,\dot{\underline{\mathbf{u}}}_P^c+\alpha\,\underline{\mathbf{C}}_{XF}\,\dot{\underline{\mathbf{u}}}_F^p+\alpha\,\underline{\mathbf{C}}_{XX}\,\dot{\underline{\mathbf{u}}}_X^p+\alpha\,\underline{\mathbf{C}}_{XP}\,\dot{\underline{\mathbf{u}}}_P^p\\&-(1+\alpha)\,\underline{\mathbf{K}}_{XP}\,\underline{\mathbf{u}}_P^c+\alpha\,\underline{\mathbf{K}}_{XF}\,\underline{\mathbf{u}}_F^p+\alpha\,\underline{\mathbf{K}}_{XX}\,\underline{\mathbf{u}}_X^p+\alpha\,\underline{\mathbf{K}}_{XP}\,\underline{\mathbf{u}}_P^p\\&+\underline{\mathbf{M}}_{XF}\left[A_0\,\underline{\mathbf{u}}_F^p+A_2\,\dot{\underline{\mathbf{u}}}_F^p+A_3\,\ddot{\underline{\mathbf{u}}}_F^p\right]+\underline{\mathbf{M}}_{XX}\left[A_0\,\underline{\mathbf{u}}_X^p+A_2\,\dot{\underline{\mathbf{u}}}_X^p+A_3\,\ddot{\underline{\mathbf{u}}}_X^p\right]\\&+(1+\alpha)\,\underline{\mathbf{C}}_{XF}\left[A_1\,\underline{\mathbf{u}}_F^p+A_4\,\dot{\underline{\mathbf{u}}}_F^p+A_5\,\ddot{\underline{\mathbf{u}}}_F^p\right]+(1+\alpha)\,\underline{\mathbf{C}}_{XX}\left[A_1\,\underline{\mathbf{u}}_X^p+A_4\,\dot{\underline{\mathbf{u}}}_X^p+A_5\,\ddot{\underline{\mathbf{u}}}_X^p\right]\end{aligned} \tag{12}$$

$$A_0=\frac{1}{\beta\Delta t^2}\qquad A_1=\frac{\gamma}{\beta\Delta t}\qquad A_2=\frac{1}{\beta\Delta t} \tag{13}$$

$$A_3=\frac{1}{2\beta}-1\qquad A_4=\frac{\gamma}{\beta}-1\qquad A_5=\Delta t\left(\frac{\gamma}{2\beta}-1\right)$$

In matrix notation, Eq.s (7) and (8) become

$$\begin{bmatrix} \overline{\underline{\mathbf{K}}}_{FF} & \overline{\underline{\mathbf{K}}}_{FX} & (1+\alpha)\,\underline{\mathbf{d}}_{FX} \\ \overline{\underline{\mathbf{K}}}_{XF} & \overline{\underline{\mathbf{K}}}_{XX} & -(1+\alpha)\,\underline{\mathbf{I}}_{XX} \end{bmatrix} \begin{bmatrix} \underline{\mathbf{u}}_F^c \\ \underline{\mathbf{u}}_X^c \\ \underline{\mathbf{X}}_X^c \end{bmatrix} = \begin{bmatrix} \overline{\underline{\mathbf{F}}}_F \\ \overline{\underline{\mathbf{F}}}_X \end{bmatrix} \tag{14}$$

In all the interaction degrees of freedom, and for the current time step $(t+\Delta t)$, a compatibility equation is required. The subtraction between a displacement of the vehicle and the corresponding displacement of the structure must be equal to the gap g_i (see Figures 1 and 2). This compatibility equation can be written as

$$\underline{\mathbf{u}}_X^c - \underline{\mathbf{u}}_Y^c = \underline{\mathbf{g}}_X^c \tag{15}$$

being

$$\underline{\mathbf{u}}_Y^c = \underline{\mathbf{c}}_{YF}\ \underline{\mathbf{u}}_F^c + \underline{\mathbf{c}}_{YP}\ \underline{\mathbf{u}}_P^c + \underline{\mathbf{f}}_{YY}\ \underline{\mathbf{Y}}_Y^c \tag{16}$$

In this equation, each component c_{ij} of $\underline{\mathbf{c}}_{YF}$ corresponds to the displacement in the Y type degree of freedom i for a single unit displacement in the F type degree of freedom j (see Figure 2). The components of matrix $\underline{\mathbf{c}}_{YP}$ have a similar meaning. Each component f_{ij} of $\underline{\mathbf{f}}_{YY}$ corresponds to the displacement in the Y type degree of freedom i for a single load consisting of a unitary force on the Y type degree of freedom j (see Figure 2). All the components of the matrix $\underline{\mathbf{f}}_{YY}$ are calculated assuming null generalized displacements in the F type and P type degrees of freedom. When the finite elements are based on the beam theory the $\underline{\mathbf{f}}_{YY}$ matrix is not null. In finite elements whose formulation is based on shape functions the $\underline{\mathbf{f}}_{YY}$ matrix is null.

Since the number of Y type degrees of freedom coincides with the number of X type degrees of freedom, the subscript Y may be replaced with X. According to [4], Eq. (15) is equivalent to

$$(1+\alpha)\,\underline{\mathbf{c}}_{XF}\ \underline{\mathbf{u}}_F^c - (1+\alpha)\,\underline{\mathbf{u}}_X^c - (1+\alpha)\,\underline{\mathbf{f}}_{XX}\ \underline{\mathbf{X}}_X^c = -(1+\alpha)\,\underline{\mathbf{g}}_X^c - (1+\alpha)\,\underline{\mathbf{c}}_{XP}\ \underline{\mathbf{u}}_P^c \tag{17}$$

Rewriting Eq.s (14) and (17) in matrix form leads to

$$\begin{bmatrix} \overline{\underline{\mathbf{K}}}_{FF} & \overline{\underline{\mathbf{K}}}_{FX} & (1+\alpha)\,\underline{\mathbf{d}}_{FX} \\ \overline{\underline{\mathbf{K}}}_{XF} & \overline{\underline{\mathbf{K}}}_{XX} & -(1+\alpha)\,\underline{\mathbf{I}}_{XX} \\ (1+\alpha)\,\underline{\mathbf{c}}_{XF} & -(1+\alpha)\,\underline{\mathbf{I}}_{XX} & -(1+\alpha)\,\underline{\mathbf{f}}_{XX} \end{bmatrix} \begin{bmatrix} \underline{\mathbf{u}}_F^c \\ \underline{\mathbf{u}}_X^c \\ \underline{\mathbf{X}}_X^c \end{bmatrix} = \begin{bmatrix} \overline{\underline{\mathbf{F}}}_F \\ \overline{\underline{\mathbf{F}}}_X \\ \overline{\underline{\mathbf{g}}}_X \end{bmatrix} \tag{18}$$

being

$$\overline{\underline{\mathbf{g}}}_X = -(1+\alpha)\,\underline{\mathbf{g}}_X^c - (1+\alpha)\,\underline{\mathbf{c}}_{XP}\ \underline{\mathbf{u}}_P^c \tag{19}$$

It is possible to demonstrate that in Eq. (18) the coefficient matrix of the system of linear equations is symmetric.

3. APPLICATION TO THE DYNAMIC ANALYSIS OF THE SÃO LOURENÇO BRIDGE

3.1 Dynamic model of the bridge

The bridge is located at the km +158.662 of the North Line of the Portuguese railway system, in a recently upgraded section for the passage of the Alfa pendular train at a maximum speed of 220 km/h.

The bridge is a bowstring arch composed of two half-decks spanning 42 m with a single track in each [5]. Figure 3 shows a view of the bridge. Each deck consists of a 40 cm thick prestressed concrete slab suspended by two lateral arches (see Figure 4). The arches are linked in the upper part by transversal girders with a rectangular hollow section and diagonals in double angles that assure the bracing of the arches.

Figure 3. São Lourenço bridge

The bridge was modeled with 2D beam elements. The influence of the deck-track composite effect in the dynamic behavior of railway bridges, due to the transmission of shear stresses between the deck and the rails at the ballasted layer, was treated in [6] and considered in the current finite element model (see Figure 4).

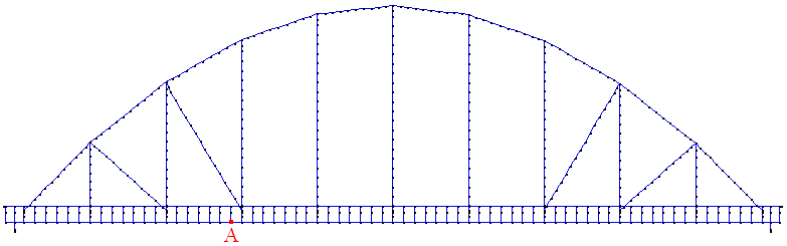

Figure 4. FEM model of the bridge

The first three vertical mode shapes of the bridge (1V, 2V and 3V) are represented in Figure 5.

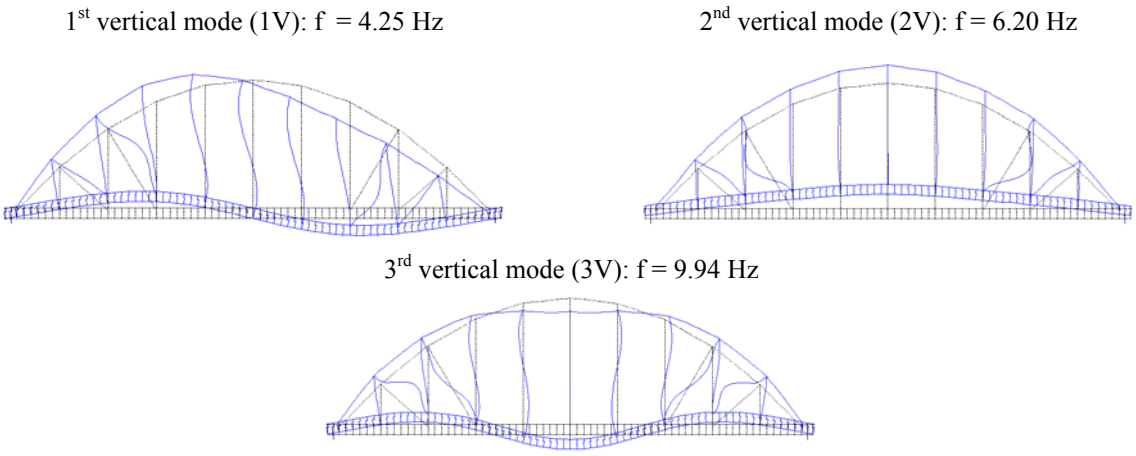

Figure 5. Mode shapes and corresponding frequencies

3.2 Dynamic model of the Alfa pendular train

The Alfa pendular train is composed of six carriages. Each carriage has two bogies with two axles each (Figure 6). The total weight of the composition is 298.3 t, tare weight, and 323.3 t for a regular loading. The maximum weight per axle is 14.4 t and the total length of the composition is 158.90 m.

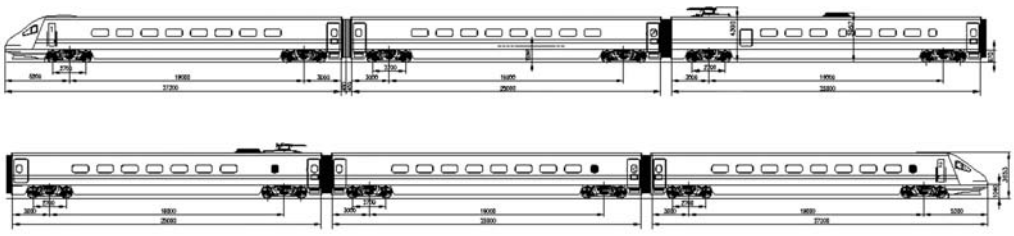

Figure 6. Alfa pendular train

The dynamic model of the train is shown in Figure 7 and consists of rigid bodies simulating the vehicle box (mass M_c) and the bogies (mass M_b), springs with stiffness K_p (or K_s) and dashpots with damping c_p (or c_s) simulating the primary (or secondary) suspensions, springs with stiffness K_h simulating the wheel-rail contact and masses M_e simulating the axles and wheels. The train is modeled with 2D beam elements (see Figure 7).

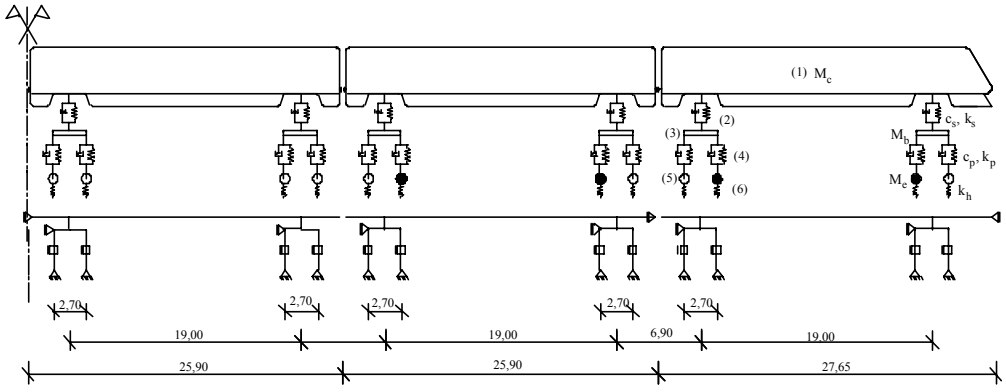

Figure 7. Dynamic model of the Alfa pendular train

3.3 Comparison between numerical and experimental results

In order to validate the numerical model an experimental campaign was undertaken, which included an ambient vibration test and several measurements of passages of the Alfa pendular train [6]. The ambient vibration test was used to identify the dynamic properties of the structure, namely its natural frequencies, mode shapes and damping coefficients. The vertical accelerations at some points of the deck were measured during several passages of the Alfa pendular train. A good agreement between the natural frequencies obtained with the numerical model and the experimental values can be observed (see Table 1).

Mode	Frequency (Hz)	
	Experimental	Numerical
1V	4.49	4.25 (-5.4%)
2V	6.05	6.20 (+2.5%)
3V	9.96	9.94 (-0.2%)

Table 1: Experimental and numerical natural frequencies

A dynamic analysis considering the train-bridge interaction was performed using the HHT method with constant average acceleration, i.e., with $\alpha = 0$, $\beta = 1/4$ and $\gamma = 1/2$ [7] and a time step equal to 0.002 s. Rayleigh damping is adopted in the present study. The damping ratios of modes 1V and 3V are equal to 1.4% and 2.4%, respectively (see Table 1).

Figure 8 compares the numerical and experimental results obtained for the vertical acceleration of the deck at point A (see Figure 4), for the passage of the Alfa pendular train at 155 km/h. Both results are filtered by means of a low-pass Chebyshev (type II) filter with a cut-off frequency of 30 Hz, in accordance with the recommendations of EN1990-A2 [8].

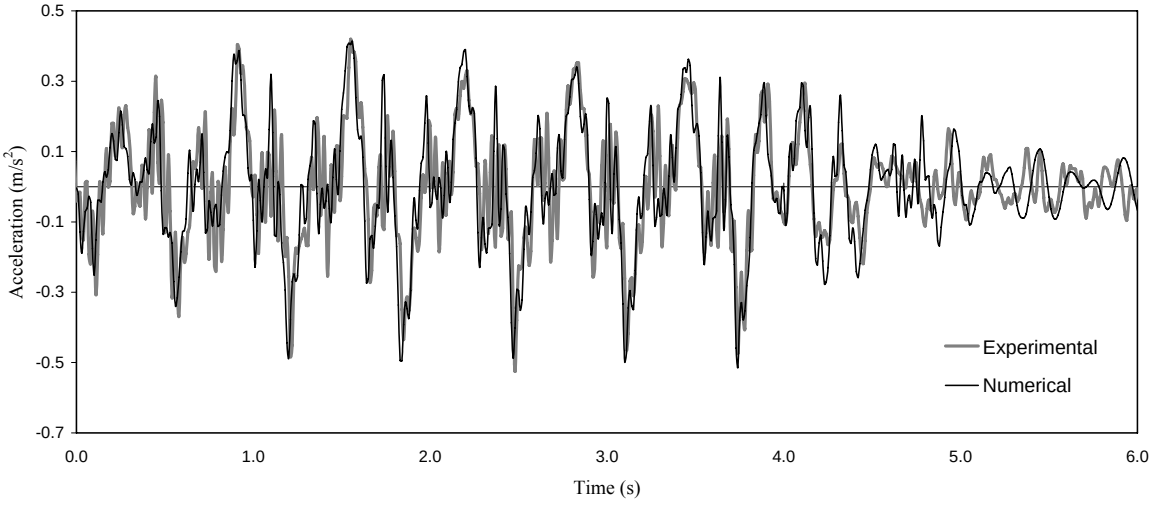

Figure 8. Vertical acceleration of the deck for the passage at 155 km/h

3.4 Dynamic response of the train-bridge system

Several dynamic analyses were performed for speeds ranging between 140 an 420 km/h, with a 5 km/h step, consisting of 57 simulated passages.

Figure 9 shows the time histories of the vertical acceleration at the span quarter-point for the passage of the Alfa pendular train at 155 km/h and 395 km/h, and at mid-point, at 155 km/h and 295 km/h.

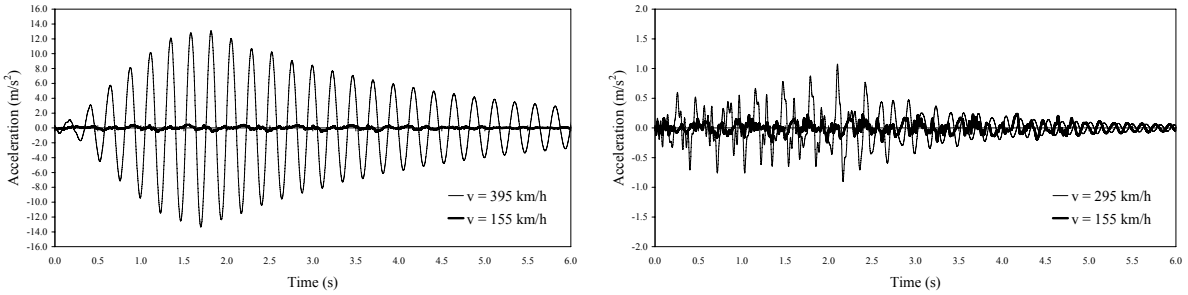

a) b)

Figure 9. Vertical acceleration: a) quarter-point; b) mid-point

Figure 10 shows the maximum vertical acceleration for speeds ranging between 140 and 420 km/h.

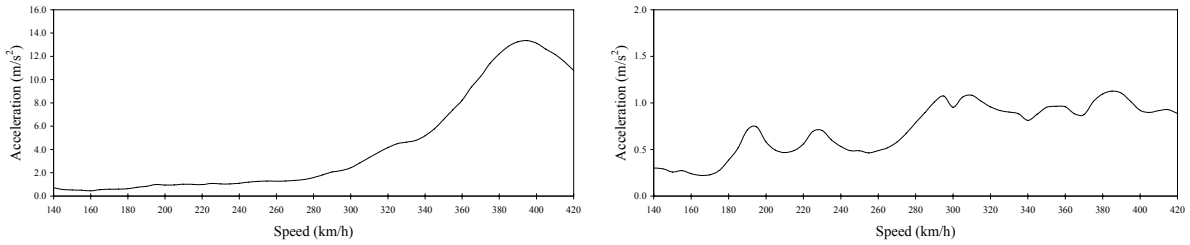

a) b)

Figure 10. Maximum vertical acceleration: a) quarter-point; b) mid-point

Resonance peaks can be observed in Figure 10 for train speeds of 395 km/h, at the span quarter-point, and for train speeds of 195 km/h, 230 km/h, 295 km/h and 310 km/h, at mid-point.

The resonance phenomena may occur for trains with regularly spaced axles, traveling at critical speeds defined by [9]

$$v_{res}(i,j) = \frac{d\, n_j}{i},\ i = 1,2,3,4,...,1/2,1/3,1/4,... \tag{20}$$

where d is the characteristic length and n_j is the jth natural frequency of the bridge. The characteristic length is a distance (many times repeated) between the vehicles or axles, that at some critical speeds may induce a periodic excitation of the bridge and cause the resonance phenomenon.

The characteristic length of the Alfa pendular train is 25.9 m (see Figure 7). According to Figure 10 and to Eq. (20), the critical speeds are: i) taking into consideration the span quarter-point and an excitation of the structure with a frequency which is equal to the mode 1V frequency (v_{res} = 25.9×4.25/1×3.6 = 396 km/h ≈ 395 km/h); ii) considering the mid-point and an excitation with a frequency which is equal to 1/2 and 1/3 of the frequency of mode 2V (v_{res} = 25.9×6.20/2×3.6 = 289 km/h ≈ 295 km/h and v_{res} = 25.9×6.20/3×3.6 =

193 km/h ≈ 195 km/h) and 1/3 and 1/4 of the frequency of mode 3V (v_{res} =25.9×9.94/3×3.6 = 309 km/h ≈ 310 km/h and v_{res} = 25.9×9.94/4×3.6 = 232 km/h ≈ 230 km/h).

The consideration of the train-bridge interaction in the dynamic analysis is particularly useful since it allows for an accurate evaluation of the vibrations of the rail cars, and, consequently, for an assessment of the riding comfort of the passengers. Figure 11 shows the time histories of the vertical acceleration in the first and last car bodies at a speed of 155 km/h, for which there is no resonance, and at a speed of 395 km/h, for which resonance of mode 1V occurs.

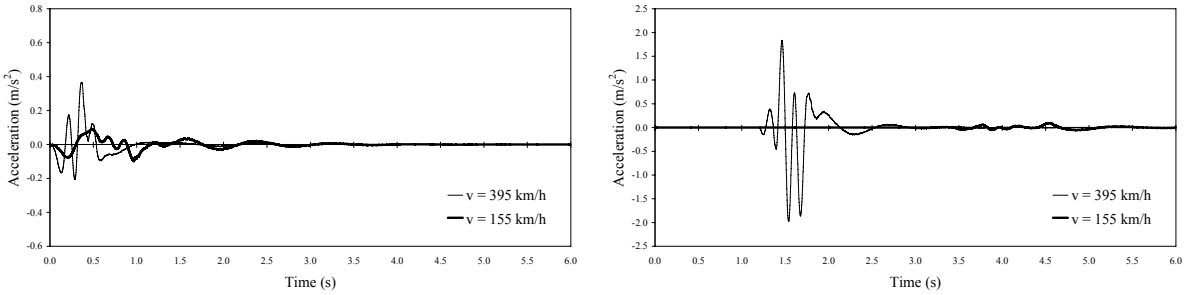

Figure 11. Vertical acceleration: a) first car body; b) last car body

Figure 12 shows the maximum vertical acceleration in the first and last car bodies of the train for speeds ranging between 140 and 420 km/h. The maximum level of acceleration occurs in the last car body for speeds that correspond to the resonance of the bridge.

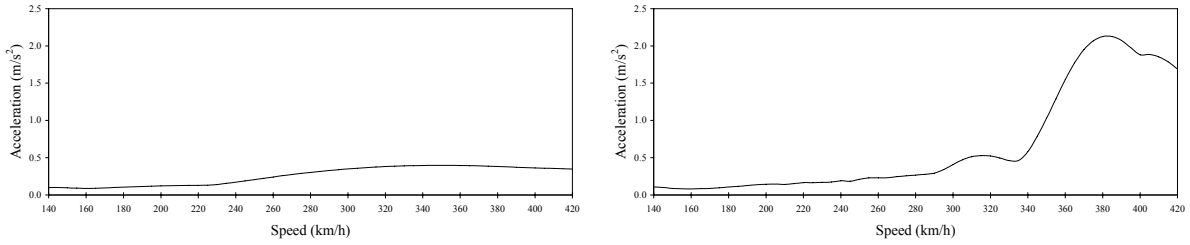

Figure 12. Maximum vertical acceleration: a) first car body; b) last car body

The dynamic analyses with train-bridge interaction were performed for 57 different speeds, which corresponded to a total execution time of 2624 s (≈44 min) in a 2.13 GHz personal computer. The bridge submesh has 1860 non prescribed degrees of freedom and the train submesh has 192. The total execution time of each analysis corresponds to the period between the entry of the first axle in the bridge and the exit of the last axle.

4. CONCLUSIONS

In the present work an integrated model whose aim is the dynamic analysis of structures by the Hilber Hughes Taylor method is proposed. This algorithm treats the interaction between moving vehicles and a structure such as a bridge. This work provides a significant improvement relatively to the method proposed in [1] and [2], since the compatibility between vehicle and structure is no longer imposed by an iterative method, but by means of an integrated formulation that considers as variables displacements and contact forces. The

governing system of equations comprises dynamic equilibrium equations and compatibility equations. The system of linear equations that arises at each time step is efficiently solved by Gaussian elimination, by considering several submatrices and their own characteristics.

The proposed formulation is applied to the dynamic behavior of a bowstring arch bridge. The numerical model was validated with the experimental results of the ambient vibration test and those measured during several passages of the Alfa pendular train. The dynamic response of the train-bridge system was calculated for train speeds only occurring in high-speed lines, allowing for a better understanding of the behavior of the system and its resonance effects. A significant improvement in terms of efficiency could also be observed.

ACKNOWLEDGMENTS

The authors wish to acknowledge the support provided by RAVE in the context of the protocol between RAVE and FEUP. This paper reports research developed under financial support provided by "FCT - Fundação para a Ciência e Tecnologia", Portugal.

REFERENCES

[1] R. Moreno Delgado, S. M. dos Santos R. C., Modelling of railway bridge-vehicle interaction on high-speed tracks. *Computers and Structures*, 63, 511-523, 1997.

[2] R. Calçada, Dynamic effects on bridges due to high-speed railway traffic. *MSc Thesis*, *Faculty of Engineering of the University of Porto (in Portuguese)*, 1995.

[3] A.F.M. Azevedo, J.A.O. Barros, J.M. Sena-Cruz, A. Ventura-Gouveia, Educational software for the design of structures. *Proceedings of the III Engineering Luso-Mozambican Congress*, *Maputo, Mozambique, 2003*, pp. 81-92 (in Portuguese), 2003. http://civil.fe.up.pt/alvaro/pdf/2003_Mocamb_Soft_Ens_Proj_Estrut.pdf

[4] A. Azevedo, S. Neves, R. Calçada, Dynamic analysis of the vehicle-structure interaction: a direct and efficient computer implementation. *Proceedings of CMNE 2007 - Congress on Numerical Methods in Engineering and XXVIII CILAMCE - Iberian Latin-American Congress on Computational Methods in Engineering, FEUP*, *Porto, Portugal*, *2007*, pp. 123 (Abstract) + 16 pages (Paper n. 1046 published on CD-ROM by APMTAC), 2007.

[5] REFER, E.P – Rede Ferroviária Nacional, Replacement of the S. Lourenço bridge at km 158,662. Design Project – Project brief, *Lisboa*, 2003.

[6] D. Ribeiro, R. Calçada, R. Delgado, Experimental calibration of the numerical model of the S. Lourenço railway bridge. VI Conference on Steel and Composite Construction, *Porto, Portugal* (in Portuguese), 2007.

[7] T.J.R. Hughes, *The Finite Element Method*. Dover Publications, Inc, New York, 2000.

[8] EN1990-A2, Annex A2: Application for Bridges. *European Committee for Standardization (CEN), Brussels*, 2005.

[9] EN1991-2, Actions on Structures – Part 2: General Actions – Traffic loads on bridges. *European Committee for Standardization (CEN), Brussels*, 2003.